



Kahramanmaraş Sütçü İmam University Journal of Engineering Sciences



Geliş Tarihi : 17.02.2025
Kabul Tarihi : 28.02.2025

Received Date : 17.02.2025
Accepted Date : 28.02.2025

A STUDY ON THE MECHANICAL PROPERTIES OF PLA+ SAMPLES MANUFACTURED USING 3D PRINTING WITH DIFFERENT RASTER ANGLES

FARKLI YAZDIRMA AÇILARI İLE 3D YAZICI KULLANILARAK ÜRETİLEN PLA+ NUMUNELERİNİN MEKANİK ÖZELLİKLERİ ÜZERİNE BİR ÇALIŞMA

Mete Han BOZTEPE¹ (ORCID: 0000-0001-8418-1352)

¹ Şırnak Üniversitesi, Makine Mühendisliği Bölümü, Şırnak, Türkiye

*Sorumlu Yazar / Corresponding Author: Mete Han BOZTEPE, metehanboztepe@snr.edu.tr

ABSTRACT

In this study, the mechanical properties of PLA+ samples produced with different raster angles (0°, 90°, 0°/90°, 45° and ±45°) were investigated. Tensile tests were performed to determine the mechanical properties according to ASTM D-638 standard. The effects of raster angle on mechanical properties such as maximum force, elongation, toughness, modulus of elasticity, and ultimate tensile strength were analyzed. The results show that the raster angle significantly affects the mechanical behavior of PLA+ specimens. The highest maximum force and ultimate tensile strength were observed at 90°. In contrast, the lowest mechanical values were recorded at 0°, indicating a decrease in strength in this configuration. The ±45° raster angle exhibited the highest elongation and toughness, indicating greater ductility and energy absorption capacity. The modulus of elasticity showed relatively small differences between the different raster angles, with the highest value recorded at 90°. These findings highlight the critical role of raster angle selection in optimizing the mechanical performance of PLA+ components and provide valuable insights for additive manufacturing applications.

Keywords: 3D printing, pla+, raster angle, tensile test

ÖZET

Bu çalışmada, farklı yazdırma açıları (0°, 90°, 0°/90°, 45° ve ±45°) ile üretilen PLA+ numunelerinin mekanik özellikleri incelenmiştir. Mekanik özellikleri belirlemek için ASTM D-638 standardına uygun olarak çekme testleri gerçekleştirilmiştir. Yazdırma açısının maksimum kuvvet, uzama, tokluk, elastikiyet modülü ve nihai çekme mukavemeti gibi mekanik özellikler üzerindeki etkileri analiz edilmiştir. Sonuçlar, yazdırma açısının PLA+ numunelerinin mekanik davranışını önemli ölçüde etkilediğini göstermektedir. En yüksek maksimum kuvvet ve nihai gerilme mukavemeti 90°'de gözlenmiştir. Buna karşılık, en düşük mekanik değerler 0°'de kaydedilmiştir, bu da bu konfigürasyonda mukavemette bir düşüş olduğunu göstermektedir. ±45° tarama açısı, daha fazla süneklik ve enerji emme kapasitesine işaret eden en yüksek uzama ve tokluğu sergilemiştir. Elastisite modülü, farklı yazdırma açıları arasında nispeten küçük farklılıklar göstermiş ve en yüksek değer 90°'de kaydedilmiştir. Bu bulgular, PLA+ bileşenlerinin mekanik performansını optimize etmede yazdırma açısı seçiminin kritik rolünü vurgulamakta ve eklemeli üretim uygulamaları için değerli bilgiler sağlamaktadır.

Anahtar Kelimeler: 3B yazıcı, pla+, yazdırma açısı, çekme testi

INTRODUCTION

Nowadays, it has become possible to develop flexible and complex-shaped products thanks to additive manufacturing (AM). This manufacturing method allows the production of parts that are difficult to produce with high dimensional accuracy compared to traditional manufacturing. It also offers a low-cost, fast manufacturing process and high efficiency. There are various methods in the AM, such as Vat Photopolymerization, Material Extrusion, Material Spraying, Powder Bed Fusion, Sheet Lamination, Binder Spraying, and Direct Energy Deposition. Although plastics, polymers, thermosets, liquids, and powders are used in the layer-by-layer production method, there is still a limited variety of materials. The 3D printing method is one of the additive manufacturing methods. This technique makes it possible to produce rapid prototyping and complex parts. 3D printing is used in many areas such as automotive, aviation, and construction (Lalegani & Mohd Ariffin, 2020). In 3D printing technology, the part is designed with computer-aided software (CAD) and produced layer by layer. This technology provides flexible production and convenience in many areas. The most commonly used materials in 3D printing are thermoplastics, ceramics, graphene-derived materials, and metallic materials (Shahrubudin et al., 2019). 3D prints produced with metal materials are generally used in areas such as automotive and marine (Duda & Raghavan, 2016). The most preferred materials in medical applications are ceramics and biomaterials. In addition, smart materials are developed and used with this technology today (Kessler et al., 2020; Lee et al., 2017). There are subtypes of 3D printing technology. One of them is Stereolithography (SLA). With this technique, it is possible to produce parts with high dimensional precision with the help of photocuring (Bagheri & Jin, 2019; Quan et al., 2020). Another technique is Fused Deposition Modeling (FDM). In this technique, thermoplastic materials are printed layer by layer with the help of heat. The selective Laser Sintering (SLS) technique is three-dimensional objects obtained by sintering particulate materials layer by layer using a laser (Chia & Wu, 2015). 3D printing technology has revolutionized many products. It is used in the production of lightweight and complex parts in the aerospace and automotive industries (Duda & Raghavan, 2016). In the energy storage field, devices' performance is increased with precise control of electrodes and electrolytes (Zhang et al., 2017). In addition, 3D printing plays an important role in producing customized agricultural and food products in the farming and food sectors (Shahrubudin et al., 2019).

The mechanical properties of the filaments used in the FDM method directly affect the mechanical properties of the final product. These mechanical properties vary depending on building orientation, raster angle/orientation, layer thickness, and infill percentage. It is possible to determine these mechanical properties with the help of tensile tests. Generally, ASTM D638 and ISO 527 standards are preferred for tensile tests (Çakan, 2021). Ayatollahi et al. conducted tensile and fracture strength tests to determine the mechanical properties of samples produced from PLA filaments. For this purpose, they produced samples with four different raster angles (0/90°, 15/-75°, 30/-60°, and 45/-45°). Specimens with 45/-45° raster angles exhibited maximum percentage elongation and fracture strength compared to specimens with other raster angles. The critical J-integral of the 45/-45° specimen was 6815 J/m², while this value was 1839 J/m² for the 0/90° specimen (Ayatollahi et al., 2020). Verma et al. conducted a similar study for samples obtained from ABS filaments. They used three raster angles (0°, +45/-45°, and 90°). They reported that the samples with +45/-45° raster angle had high fracture strength (Verma et al., 2021). In another study, the mechanical properties of PLA and PETG samples with 15° - 30° raster angles were investigated. It was indicated that the raster angle affects the mechanical properties of both material types. The data obtained from the mechanical tests were compared with the study simulated with ANSYS software, and the maximum matching was obtained from the PLA sample with 15° raster angle (Albadrani, 2023). When PLA samples with 0° and 90° raster angles were subjected to tensile testing, the highest tensile strength was obtained with the sample with 0° raster angle (Rajpurohit & Dave, 2019).

The tensile properties of polylactic acid (PLA) and its composites have been extensively studied, revealing significant insights into their mechanical performance and potential applications. PLA, a biodegradable thermoplastic derived from renewable resources, exhibits high tensile strength, typically ranging from 50 to 70 MPa, and a Young's modulus around 3 GPa at room temperature (Aliotta et al., 2019). However, its inherent brittleness limits its applications, necessitating the incorporation of various fillers and reinforcements to enhance its mechanical properties (Kangwanwathanasiri et al., 2013). The tensile testing of Polylactic Acid (PLA) and its composites is a critical area of research in materials science, particularly due to PLA's increasing use in additive manufacturing and its biodegradable properties. PLA exhibits a range of tensile strengths depending on its formulation and processing conditions. For instance, Vakharia et al. report that the ultimate tensile strength of pure PLA can range between 45 and 50 MPa, while variations such as MI-PLA show strengths between 35 and 40 MPa (Vakharia et al., 2021).

In this study, the effect of specimens with different raster angles on mechanical properties was investigated. The tensile strengths of specimens with raster angles of 0° , 90° , $0^\circ/90^\circ$, 45° , and $\pm 45^\circ$ produced by the FDM technique using PLA+ filaments were determined. Test specimen dimensions were prepared according to ASTM D 638 standard type 1.

MATERIALS AND METHODS

Material

PLA is a frequently used filament in FDM applications due to its environmentally friendly and biodegradable properties. It is also made from renewable resources, so the energy consumed in processing is low. It is used in rapid prototyping and many other applications. However, its mechanical weaknesses and other limitations are being overcome with innovative approaches such as composite materials and surface modifications. These developments allow PLA to be used in a wider range of applications. There are some key differences between PLA (Polylactic Acid) and PLA+ (PLA Plus) filaments. PLA+ is an enhanced version of PLA and offers better performance properties, usually through the addition of various additives. The properties of the PLA+ filament used in this research are given in Table 1. This filament is a product of the eSUN brand. PLA+ is preferred for more durable mechanical parts or applications requiring flexibility and durability.

Table 1. Properties of PLA+ material

Density (g/cm ³)	1.23
Tensile Strength (MPa)	60
Flexural Strength (MPa)	74
Flexural Modulus (MPa)	1973
Elongation at Break (%)	20
Extruder Temperature (°C)	210-230
Bed Temperature (°C)	45-60
Printing Speed (mm/s)	40-100

Specimen Design

The specimens were printed in a dogbone shape to test the tensile strength according to ASTM D-638. The specimen dimensions were set according to type 1 with a thickness of 3 mm and a length of 165 mm. The shape of a specimen and other dimensions are given in Figure 1.

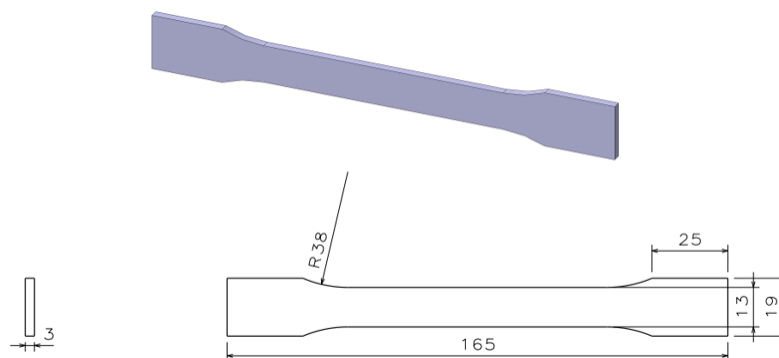


Figure 1. Dimensions of the test specimen according to ASTM D-638

The 3D-Printing Process

3D modeling of the test specimens was designed with CATIA software. The 3D model was converted to STL format for physical printing on the 3D printer. The STL file was then transferred to the computer controlling the 3D printer. As shown in Figure 2, a dogbone specimen was visualized on the 3D printer interface using Cura 5.9.0 software. With this software, parameters such as table and nozzle temperature, print speed, scan angle, and infill density can be easily adjusted. In this study, the table temperature was set to 50 °C, and the nozzle temperature was set to 210 °C. The printing speed was 50 mm/s, and the infill density was 100%. Five angles were used to examine the tensile strength of the specimens depending on the raster angles. These are 0°, 90°, 0°/90°, 45°, ±45° respectively. The raster angles are given in Figure 3.

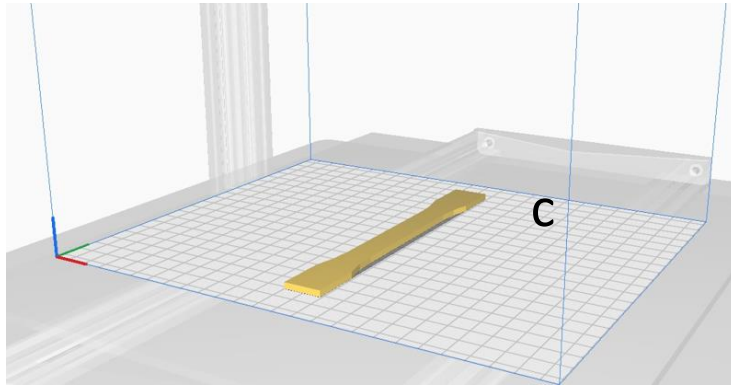


Figure 2. Dogbone specimen on 3D printer image captured from software Cura 5.9.0

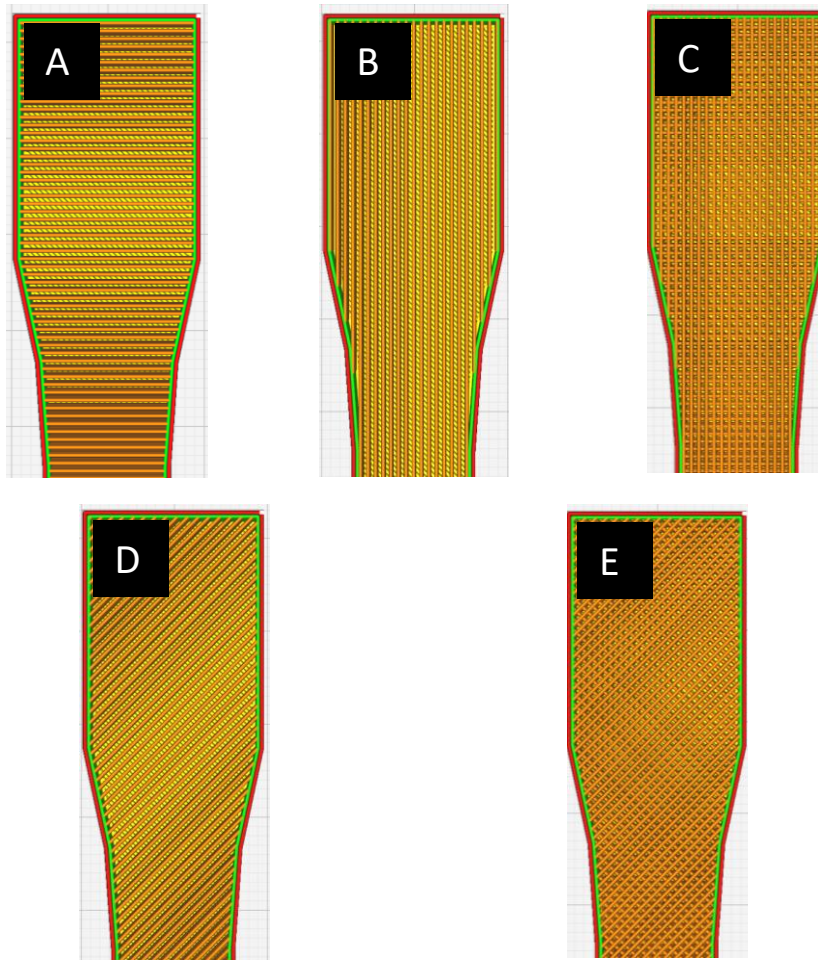


Figure 3. Raster angles of specimens (a) 0°, (b) 90°, (c) 0°/90°, (d) 45°, (e) ±45°

RESULTS AND DISCUSSION

Tensile Test

All the tensile test specimens were tested according to the ASTM D638 standard testing method for plastic material. A universal tensile testing machine with a capacity of 100 kN was used to determine the mechanical properties. The displacement during the test was obtained from data from an extensometer placed on the specimen. To repeat the tests, 2 pieces of each sample were produced and tested at a speed of 5 mm/min.

Toughness is considered the ability of a material to resist tearing or breaking due to tensile load. The term toughness most commonly refers to the energy that a material absorbs as it fractures, and it is the material's modulus of toughness. In materials, stress, and strain curves for tensile tests, the maximum area under the curves measures the modulus of toughness.

Figure 4 shows a graph of the tensile result. In addition, the tensile test results given in Table 2 show the effect of the raster angle used on the mechanical performance of PLA+ specimens. By comparing the maximum force, elongation, and average values of the specimens tested at different raster angles, important findings were obtained about the load-carrying capacity and ductility of the material.

Specimens with 90° raster angle show the highest strength with an average maximum force of 1774.18 N. However, the elongation values are low and average 0.775 mm. This indicates that the material exhibits a more brittle behavior in this direction. The specimens with 0° raster angle have the lowest maximum force value (average 1314.29 N). Also, the elongation values are relatively low, averaging 0.66 mm. This indicates that specimens printed in this orientation have low load-carrying capacity. The combination of 0°/90° angles shows better mechanical performance compared to the 0° angle alignment, with an average maximum force of 1623.32 N. Elongation values are also slightly higher, with 0.91 mm. This combination offers more stable mechanical properties compared to the 0° orientation. The specimens printed with a 45° raster angle show a better load-carrying capacity compared to the specimens with a 0° raster angle, with an average force of 1571.11 N. Elongation values are 1.16 mm on average, and this orientation increases ductility. The combination with $\pm 45^\circ$ Raster Angle shows the highest ductility. The average maximum force is 1746.85 N, and the elongation value reaches up to 3.68 mm. This result shows that the cross-oriented fibers provide more deformation under stress, allowing the material to absorb more energy before fracture.

The data obtained show that the raster angle has a significant effect on the mechanical properties of PLA+ material. Specimens with a raster angle of 90° have the highest strength but poor ductility. The $\pm 45^\circ$ combination has the highest elongation capacity and increases ductility, making the material more resistant to fracture.

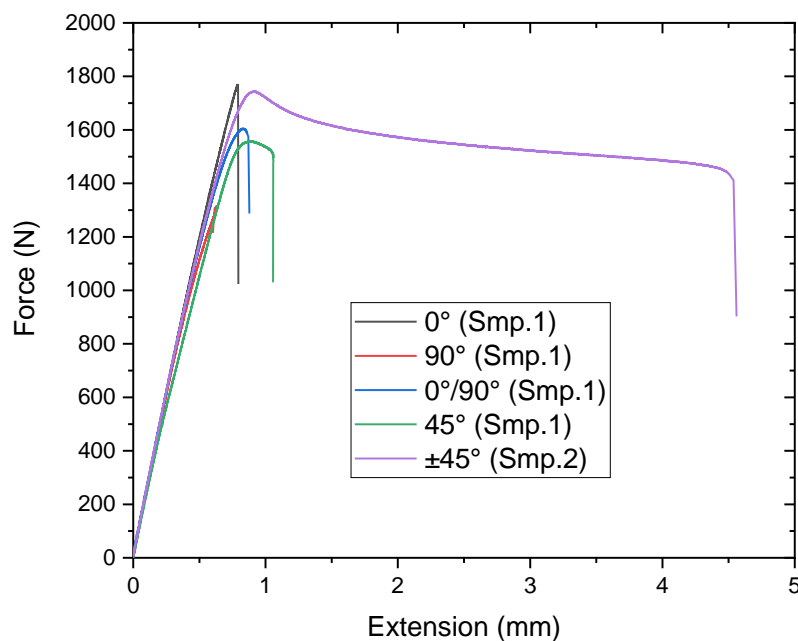


Figure 4. Force-displacement curves for tensile test of PLA+ (Smp.: Sample)

Table 2. The tensile test results for the PLA+ due to the raster angle

Raster Angle	Samples	Max. Force (N)	Extension (mm)	Average Force (N)	Average Extension (mm)
90°	1	1768.70	0.79	1774.18	0.775
	2	1779.67	0.76		
0°	1	1314.96	0.63	1314.29	0.66
	2	1313.63	0.69		
0°/90°	1	1605.32	0.87	1623.32	0.91
	2	1641.33	0.96		
45°	1	1557.51	1.06	1571.11	1.16
	2	1584.71	1.27		
±45°	1	1749.66	2.82	1746.85	3.68
	2	1744.04	4.55		

The mechanical properties presented in Table 3 show that PLA+ specimens exhibit different toughness, modulus of elasticity, and ultimate stress values depending on the raster angle. These results indicate that the material exhibits significant differences in load-carrying capacity and ductility. Stress-strain curves of the specimens are also given in Figure 5.

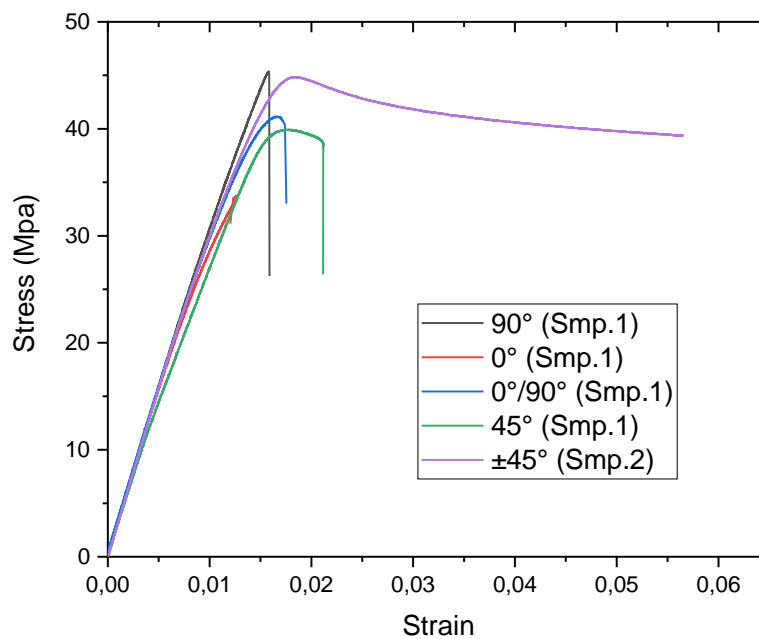
**Figure 5.** Stress-strain curves for tensile test of PLA+ (Smp.: Sample)

Table 3. Stress-strain results of PLA+ due to the raster angle

Raster Angle	Samples	Modulus Toughness (KJ/m ³)	Modulus Elasticity (GPa)	Ultimate Stress (Mpa)
90°	1	383±8.26	3.21±0.04	45.35
	2	365±6.12	3.62±0.07	45.63
0°	1	236±4.12	3.17±0.05	33.71
	2	252±5.46	3.22±0.04	33.68
0°/90°	1	433±5.28	3.25±0.08	41.16
	2	503±5.22	3.18±0.07	42.08
45°	1	547±8.45	2.88±0.06	39.93
	2	732±6.62	2.98±0.06	40.63
±45°	1	2055±13.20	3.20±0.05	44.83
	2	3352±21.32	3.21±0.06	44.71

Modulus of Toughness

The 90° raster angle specimens have a relatively high energy absorption capacity with toughness values of 383 ± 8.26 and 365 ± 6.12 kJ/m³. The specimens with 0° raster angle show the lowest toughness values of 236 ± 4.12 and 252 ± 5.46 kJ/m³. This indicates that it has a lower deformation capacity under load and exhibits a brittle structure. The 0°/90° specimens exhibit better toughness compared to the 0° specimens with values of 433 ± 5.28 and 505 ± 5.22 kJ/m³. Specimens with a raster angle of 45° show good energy absorption with a toughness value of 732 ± 6.62 kJ/m³ and 547 ± 8.45 . The ±45° combination has the highest toughness with values of 2055 ± 13.20 and 3352 ± 21.32 kJ/m³. This indicates that the cross-oriented fibers allow more deformation under load, and the material exhibits ductile behavior.

Modulus of Elasticity

The modulus of elasticity values are between 2.88 GPa and 3.62 GPa. The 90° specimens have the highest modulus of elasticity (3.21-3.62 GPa). This shows that the stiffness of the material increases with this raster angle. The 0° raster angle specimens show a modulus of elasticity between 3.17-3.22 GPa, indicating that the material's stiffness is lower than the 90° specimens. The modulus of elasticity of the 0°/90° specimens was measured as 3.25 ± 0.08 GPa and 3.18 ± 0.07 GPa, respectively. The 45° oriented specimens have the lowest value in terms of modulus of elasticity, in the range of 2.88-2.98 GPa. The ±45° specimens show a balanced modulus of elasticity with 3.20-3.21 GPa. The findings are compatible with the literature (Aliotta et al., 2019).

Ultimate Stress

The ultimate stress values ranged from 33.68 MPa to 45.63 MPa. The 90° raster angle specimens have the highest ultimate stress value of 45.35-45.63 MPa. The 0° specimens have the lowest ultimate stress value of 33.68-33.71 MPa, indicating that the fiber orientation has a lower load-carrying capacity in this direction in accordance with

(Algarni, 2021). The $\pm 45^\circ$ oriented specimens exhibit high strength with ultimate stress values of 44.71-44.83 MPa. The findings confirm test results and are compatible with the literature (Çakan, 2021).

Fracture Specimens

The fracture zones of PLA+ 3D printed specimens after tensile tests are shown in Figure 6. The 0° , 90° , and $0^\circ/90^\circ$ raster angle specimens have flat fracture surfaces perpendicular to the loading direction. However, the fracture direction of the 45° raster angle specimen has a 45° degree inclined surface. For the $\pm 45^\circ$ raster angle specimen, the fracture direction is almost perpendicular to the loading direction. Also, the fractured surfaces of the 45° and $\pm 45^\circ$ raster angle specimens have a very rough surface, while the 0° , 90° , and $0^\circ/90^\circ$ raster angle specimens have almost smooth surfaces. Such cases of fracture are linked to the orientation of the constructed layers and the melting and cooling of the PLA filament during the bonding between these layers. Due to the inherent brittleness of PLA material, no necking phenomenon was observed in any of the samples. Crack formation and propagation occurred in the middle part of some samples and in the end regions of others. These differences in the crack initiation points are related to FDM printing defects caused by various factors such as vibrations, printing errors, inhomogeneous infill density, overheating, insufficient material feeding, or air gaps. Specimens with printing flaws are susceptible to high-stress concentrations, which can initiate and propagate cracks (Algarni, 2021).

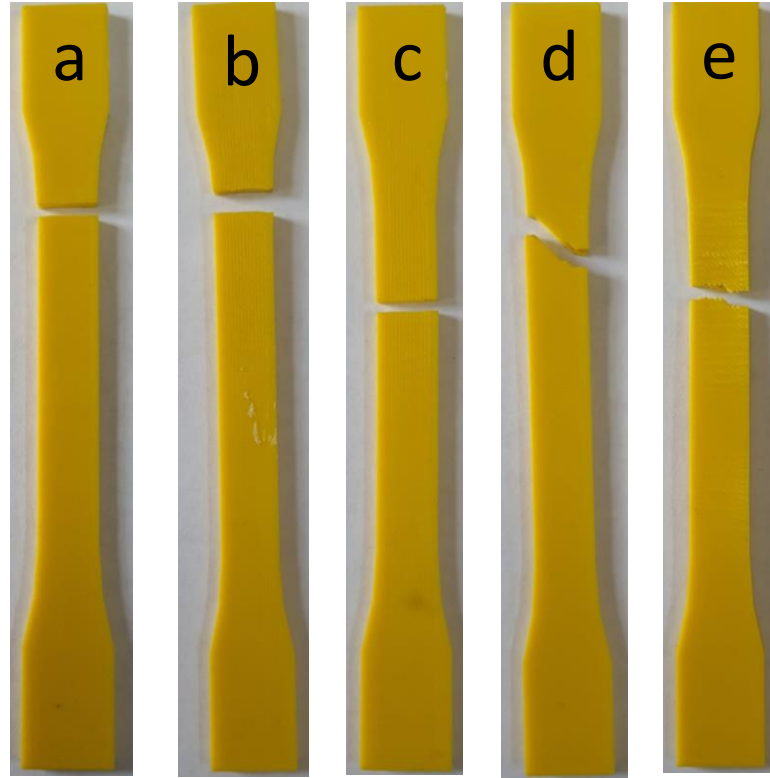


Figure 6. Specimens fractured under tensile load (a) 0° , (b) 90° , (c) $0^\circ/90^\circ$, (d) 45° , (e) $\pm 45^\circ$

CONCLUSION

In this study, the mechanical properties of PLA+ material produced at different raster angles (0° , 90° , $0^\circ/90^\circ$, 45° , $\pm 45^\circ$) were investigated by tensile testing. The specimen dimensions and tensile test were performed according to ASTM D-638 standard. As a result of the test, the effects on the toughness, modulus of elasticity, and tensile strength values of the material were investigated. The data obtained show that the raster angle has a significant effect on the mechanical properties of PLA+ specimens. Accordingly, the following findings were obtained.

- **Maximum Force:** The highest maximum force value, with an average value of 1774.18 N, was obtained at 90° raster angle. This result shows that the material has a higher load-carrying capacity at this angle. The lowest maximum force was obtained at 0° raster angle with an average value of 1314.29 N.
- **Elongation Amount:** The highest amount of elongation was obtained at the ±45° raster angle. This indicates that the material has a higher ductility at this angle. The lowest elongation was obtained at 0° raster angle.
- **Modulus of Toughness:** The highest toughness value was obtained at the ±45° raster angle. This result shows that the material has more energy absorption capacity at this angle. The lowest toughness value was obtained at 0° raster angle. This indicates that the material is more brittle at this angle.
- **Modulus of Elasticity:** The modulus of elasticity values do not vary greatly between the different raster angles. However, on average, the highest modulus of elasticity value was obtained at the 90° angle and the lowest at the 45° angle.
- **Ultimate Tensile Strength:** Tensile strength values vary depending on the raster angle. The highest tensile strength value was obtained at 90° angle. This result indicates that the material has a higher load-carrying capacity at this angle.
- **Fracture Specimens:** The fracture direction of PLA+ samples varied depending on the raster angle. Fracture surfaces were smooth in some samples and rough in others. These differences were caused by FDM printing errors and layer orientation of the material.

Acknowledgments

This study was supported by the Scientific Research Projects Coordination Unit (BAP) of Şırnak University, Şırnak, Turkey [grant number 2022.FNAP.06.05.01].

REFERENCES

- Albadrani, M. (2023). Effects of Raster Angle on the Elasticity of 3D-Printed Polylactic Acid and Polyethylene Terephthalate Glycol. *Designs*, 7. <https://doi.org/10.3390/designs7050112>
- Algarni, M. (2021). The Influence of Raster Angle and Moisture Content on the Mechanical Properties of PLA Parts Produced by Fused Deposition Modeling. *Polymers*, 13(2). doi:10.3390/polym13020237
- Aliotta, L., Gigante, V., Coltelli, M., Cinelli, P., Lazzeri, A., & Seggiani, M. (2019). Thermo-mechanical properties of pla/short flax fiber biocomposites. *Applied Sciences*, 9(18), 3797. <https://doi.org/10.3390/app9183797>
- Ayatollahi, M. R., Nabavi-Kivi, A., Bahrami, B., Yazid Yahya, M., & Khosravani, M. R. (2020). The influence of in-plane raster angle on tensile and fracture strengths of 3D-printed PLA specimens. *Engineering Fracture Mechanics*, 237, 107225. <https://doi.org/https://doi.org/10.1016/j.engfracmech.2020.107225>
- Bagheri, A., & Jin, J. (2019). Photopolymerization in 3D Printing. *ACS Applied Polymer Materials*, 1(4), 593-611. <https://doi.org/10.1021/acsapm.8b00165>
- Chia, H. N., & Wu, B. M. (2015). Recent advances in 3D printing of biomaterials. *Journal of Biological Engineering*, 9(1), 4. <https://doi.org/10.1186/s13036-015-0001-4>
- Çakan, B. G. (2021). Effects of raster angle on tensile and surface roughness properties of various FDM filaments. *Journal of Mechanical Science and Technology*, 35(8), 3347-3353. <https://doi.org/10.1007/s12206-021-0708-8>
- Duda, T., & Raghavan, L. V. (2016). 3D Metal Printing Technology. *IFAC-PapersOnLine*, 49(29), 103-110. <https://doi.org/https://doi.org/10.1016/j.ifacol.2016.11.111>
- Kangwanwatthanasiri, P., Suppakarn, N., & Ruksakulpiwat, Y. (2013). Biocomposites from cassava pulp/polylactic acid/poly(butylene succinate). *Advanced Materials Research*, 747, 367-370. <https://doi.org/10.4028/www.scientific.net/amr.747.367>
- Kessler, A., Hickel, R., & Reymus, M. (2020). 3D Printing in Dentistry—State of the Art. *Operative Dentistry*, 45(1), 30-40. <https://doi.org/10.2341/18-229-1>

- Lalegani, M., & Mohd ariffin, M. k. a. (2020). The Effects of Combined Infill Patterns on Mechanical Properties in FDM Process. *Polymers*, 12, 2792. <https://doi.org/10.3390/polym12122792>
- Lee, J.-Y., An, J., & Chua, C. K. (2017). Fundamentals and applications of 3D printing for novel materials. *Applied Materials Today*, 7, 120-133. <https://doi.org/https://doi.org/10.1016/j.apmt.2017.02.004>
- Quan, H., Zhang, T., Xu, H., Luo, S., Nie, J., & Zhu, X. (2020). Photo-curing 3D printing technique and its challenges. *Bioactive Materials*, 5(1), 110-115. <https://doi.org/https://doi.org/10.1016/j.bioactmat.2019.12.003>
- Rajpurohit, S. R., & Dave, H. K. (2019). Analysis of tensile strength of a fused filament fabricated PLA part using an open-source 3D printer. *The International Journal of Advanced Manufacturing Technology*, 101(5), 1525-1536. <https://doi.org/10.1007/s00170-018-3047-x>
- Shahrubudin, N., Lee, T. C., & Ramlan, R. (2019). An Overview on 3D Printing Technology: Technological, Materials, and Applications. *Procedia Manufacturing*, 35, 1286-1296. <https://doi.org/https://doi.org/10.1016/j.promfg.2019.06.089>
- Vakharia, V. S., Kuentz, L., Salem, A., Halbig, M. C., Salem, J. A., & Singh, M. (2021). Additive manufacturing and characterization of metal particulate reinforced polylactic acid (pla) polymer composites. *Polymers*, 13(20), 3545. <https://doi.org/10.3390/polym13203545>
- Verma, P., Ubaid, J., Schiffer, A., Jain, A., Martínez-Pañeda, E., & Kumar, S. (2021). Essential work of fracture assessment of acrylonitrile butadiene styrene (ABS) processed via fused filament fabrication additive manufacturing. *The International Journal of Advanced Manufacturing Technology*, 113(3), 771-784. <https://doi.org/10.1007/s00170-020-06580-4>
- Zhang, F., Wei, M., Viswanathan, V. V., Swart, B., Shao, Y., Wu, G., & Zhou, C. (2017). 3D printing technologies for electrochemical energy storage. *Nano Energy*, 40, 418-431. <https://doi.org/https://doi.org/10.1016/j.nanoen.2017.08.037>